Supplemental Materials

Kes1 protein purification, gel filtration and circular dichroism

His_6-Kes1 and mutant derivatives were purified from the soluble fraction of E. coli whole cell lysates prepared in lysis buffer (25mM Na_2HPO_4, 300mM NaCl, 5mM BME, pH7.5) using TALON® metal affinity resin (Clontech) and bound protein was eluted with lysis buffer containing 200mM imidazole. For gel filtration 0.5 – 1mg of protein was concentrated to 0.5ml by using a spin concentrator with an Amicon Ultracel 10K filter device (Millipore). The concentrated material was then subjected to gel filtration chromatography on a S75 (10/300) column (GE Bioscience) pre-equilibrated with buffer (25mM Na_2HPO_4, 300mM NaCl, 5mM BME, pH7.5). The fractions containing peak A_{280nm} absorbance, eluting in between 15.5 and 17.5ml were pooled and their protein content was quantified using the micro BCA method (Pierce).

For circular dichroism spectrophotometry, pooled fractions obtained after gel filtration chromatography were adjusted to 0.2mg/ml and dialyzed, twice, against 4L of 10mM potassium phosphate buffer, pH 7.5. Spectra was collected between 260-185nm on an Applied Photophysics Chirascan Plus steady state Circular Dichroism/ Fluorescence spectrometer using a 1mm path length cuvette.

Sterol binding analysis

Kes1 and mutant Kes1 sterol binding analyses were performed in a 100µl volume containing 20mM HEPES pH 7.5, 150mM KCl, 0.05% Triton X-100, 500 ng of purified protein and 0.025 - 2 µM ^{3}H-cholesterol (40 Ci/mmol, American Radiolabeled Chemicals) delivered in ethanol. For non-specific binding analyses 0 - 20µM of unlabeled

cholesterol, delivered in ethanol, was added to each reaction. Each experiment received the same amount of ethanol (2% v/v). Reactions were performed at room temperature for 3 hours after which 20 μl of TALON® metal affinity resin (50% (w/v)) (Clontech) pre-equilibrated with 20mM HEPES pH 7.5, 150mM KCl, 0.05% Triton X-100 was added and incubated for a further 30 mins. The tubes were centrifuged at 13,000g for 1 min and washed 4X with 1 ml of 20mM HEPES pH 7.5, 150mM KCl. The protein was eluted from the resin with 200 μl of 20mM HEPES pH 7.5, 150mM KCl containing 200mM imidazole. After centrifuging at 13,000g for 10 min, 100 μl of supernatant was taken and the radioactivity was measured in a liquid scintillation counter.

NMR spectroscopy, spectral processing and analysis. Yeast cells (400 OD_{600} units) were pelleted by centrifugation, washed 5X with cold PBS, and 1ml of ice-cold 50% methanol was added to the cell pellet. Cells were disrupted by 3 rounds of freeze thaw at -80°C and five rounds of bead beating (30 sec each round). Lysates were incubated for 30 minutes on dry ice, thawed for 10 minutes on ice, and extracts were clarified by centrifugation at 16,000g for 10 minutes. The methanol extract was collected and evaporated to dryness by centrifugation under vacuum.

Dried extracts were suspended in 600μL D_2O containing 0.5 mM (final concentration) trimethylsilyl-2,2',3,3'-tetradeuteropropioninc acid (TSP) and transferred to a 5.0 mm NMR tube. ^1H NMR spectra were acquired at 16.4T Varian INOVA (700 MHz ^1H, Varian Instruments) equipped with 5mm indirect cold probe. The FIDs were acquired using a one-pulse sequence with a water presaturation period, a total repetition time of 12.65s, at 64 transients. All NMR spectra were processed using ACD/ 1D NMR

Manager (version 12.0; Advanced Chemistry Development, Inc., Toronto, ON, Canada). Prior to Fourier transformation, imported FID's were zero filled to 64,000 points and an exponential line broadening of 0.1 Hz was applied. Spectra were phase and baseline corrected, and referenced to the TSP peak to 0.00 ppm. Following annotation (removal of spectral regions around water, >9.7ppm, <0.4ppm), grouped spectra were data-reduced to 250 bins using intelligent bucketing and the integrals within each bin were determined. Principal Component Analysis (PCA) was carried out using SIMCA-P (version 11.0; Umetrics, Umea, Sweden) and Pareto scaling was applied to the data prior to analysis. Individual metabolites were identified and quantified using Chenomx NMR Suite (version 5.1; Chenomx Inc., Edmonton, Canada), using TSP as a reference.

Flow cytometry. Yeast cells (5 OD_{600} units) were pelleted by centrifugation and then fixed overnight in 70% (v/v) ethanol. Next, cells were washed with 1ml of citrate buffer (50mM sodium citrate pH 7), briefly sonicated and then resuspended in 1ml of citrate buffer containing 0.25mg/ml RNase A and incubated overnight at 37^{o}C. Cells were again washed in 50mM sodium citrate pH7 and then resuspended in 1ml of 50mM sodium citrate pH7 containing 16µg/ml of propidium iodide and incubated at room temperature for 30 minutes. After washing in citrate buffer cells were analyzed on a Beckman MoFlo flow cytometer.

Supplemental Figure Legends

Supplemental Figure S1. Kes1 sterol binding mutants have biological activity, related to Figure 1. **(A)** Depiction of the Kes1 sterol binding pocket shows the T_{185} side-chain, like that of Y_{97}, to coordinate a chain of ordered water molecules that stabilizes sterol bound by Kes1. The 12HZ pdb file (Im et al., 2005) was manipulated in PyMol to generate the models. **(B)** Kes1 binding affinity for free [^{3}H]-cholesterol was determined. For specific binding, [^{3}H]-cholesterol binding was performed in the presence of 0 - 20μM of unlabeled cholesterol. Error bars indicate standard deviation. **(C)** The ability of Kes1, kes1^{Y97F}, kes1^{T185V} and kes1^{3E} to bind free [^{3}H]-cholesterol was determined. Error bars indicate standard deviation. **(D)** Gel filtration of purified Kes1, kes1^{Y97F} and kes1^{T185V}. 500μg of protein was loaded on to an S75 (10/300) column and filtered at a flow rate of 0.5ml/min. Absorbance at 280nm was monitored continuously to identify the indicated Kes1 protein. **(E)** Circular dichroism of purified Kes1, kes1^{Y97F} and kes1^{T185V} protein. 200 μg/ml of purified protein in 10mM potassium phosphate buffer pH7.5 was measured on an Applied Photophysics Chirascan Plus steady state circular dichroism/ fluorescence spectrometer using a 1mm path length cuvette. **(F)** Wild-type yeast were transformed with 0.5μg purified YCp(*URA3*), YCp(*KES1*), YCp(*kes1^{Y97F}*), YCp(*kes1^{T185V}*) or YCp(*kes1^{3E}*) as indicated. These plasmids drive Kes1 production from its natural promoter and involve only mild enhancement in expression relative to wild-type endogenous levels. Transformants were grown on uracil selective media for 72 hours at 30°C. The YCp(*URA3*) vector is a mock control.

Supplemental Figure S2. TGN/endosomal trafficking defects in the face of excessive Kes1 or its sterol-binding-defective derivatives, related to Figures 1 and 2. **(A)** Membrane and cytosol fractions were prepared from yeast induced for either P_{DOX}*::KES1* or P_{DOX}*::kes1*^{Y97F} expression. Equivalent amounts of each fraction were loaded and Kes1, Sec63 (membrane specific control) and GAPDH (cytosol specific control) were visualized by western blot analysis. The membrane:cytosolic distribution for Kes1 (35%:65%) was shifted ca. 2-fold in favor of membrane binding for the sterol-binding mutant (75%:25%). **(B)** Kes1 and its sterol binding mutants perturb amino acid uptake. Wild-type yeast (CTY182) carrying ectopic expression plasmids for driving Dox-repressible expression of the indicated Kes1 species were cultured in the presence (repressive conditions for ectopic Kes1 expression) or absence of Dox (permissive conditions for ectopic Kes1 expression) for 18 hours in minimal media lacking methionine and cysteine. Cells were subsequently radiolabeled with [^{35}S]-amino acids (TransLabel; New England Nuclear; 100 μCi/ml) for the specified times and then stopped by the addition of TCA (5% final concentration). Cell pellets were exhaustively washed with 5% TCA, solubilized and [^{35}S]-radioactivity in individual cell lysates was quantified by scintillation counting. The differences were highly significant – the 10 min and longer time points showed $p \leq 0.001$ in comparing the corresponding +Dox vs –Dox conditions. Error bars indicate standard deviation. **(C)** Kes1 and Kes1 sterol binding mutants disrupt FM4-64 trafficking through the endosomal system. Wild-type yeast carrying ectopic expression plasmids for driving Dox-repressible expression of the indicated Kes1 species were cultured in the presence (repressive conditions for ectopic Kes1 expression) or absence of Dox (permissive conditions for ectopic Kes1 expression) for 18 hours. Cells

were subsequently labeled with FM4-64 (10μM) for 5 minutes after which cells were washed with 1ml of uracil-free medium and then chased for 7.5, 15 and 30 minutes at 30°C in uracil-free medium. Chase was terminated with NaN_3/NaF (10mM final, each) and fluorescence profiles were captured. **(D)** Kes1 and Kes1 sterol binding mutants disrupt Gap1 general amino acid permease trafficking to the plasma membrane. Wild-type yeast constitutively producing a Gap1-GFP reporter, and carrying ectopic expression plasmids for driving Dox-repressible expression of the indicated Kes1 species, were cultured in the presence (repressive conditions for ectopic Kes1 expression; +) or absence of Dox (permissive conditions for ectopic Kes1 expression; -) for 18 hours.

Supplemental Figure S3. Autophagy and vacuolar hydrolase function in preservation of cell viability of Kes1-arrested cells, related to Figure 3. **(A)** Yeast strain PHY2433 and an *atg1*Δ derivative were analyzed for the effect of Kes1 expression on ALP activation. Error bars indicate standard deviation. **(B)** Atg18-GFP localization was visualized in cells cultured in the presence of NH_4^+, or cells starved for NH_4^+ for 3 hours. **(C)** Kes1 and Kes1 sterol binding mutants induce autophagy. Atg18-GFP yeast harboring ectopic expression plasmids for driving Dox-repressible expression of the indicated Kes1 species were cultured in the presence (repressive conditions for ectopic Kes1 expression) or absence of Dox (permissive conditions for ectopic Kes1 expression) for 18 hours after which Atg18-GFP profiles were imaged. **(D)** Compromised cell viability of Kes1-arrested cells in the face of chronic challenge with 1mM exogenous PMSF at 30^oC. Error bars indicate standard deviation. **(E)** Enhanced Kes1 activity (-Dox condition) rapidly reduces the viability of *pep4Δ* yeast defective in vacuolar hydrolase activities. The +Dox

condition is not permissive for ectopic Kes1 expression and represents a mock Kes1-intoxication control. Error bars indicate standard deviation.

Supplemental Figure S4. Representative ^{1}H NMR spectra, related to Figure 3. **(A)** The upfield (aromatic) and downfield (aliphatic) regions of the ^{1}H NMR spectra from extracts prepared from wild-type cells (WT), or cells with elevated Kes1 or kes1^{Y97F} (as indicated) are shown with peak assignments identifying the key amino acids described in Supplemental Figure S4A. Not all signature amino acid peaks are labeled. The spectra were scaled to Ala according to their respective concentrations (1.96 : 0.46: 0.88). **(B)** Represented amino acids were quantified from extracts prepared from wild-type cells (WT), or Kes1/kes1^{Y97F}-arrested cells. Amino acid levels of Kes1/kes1^{Y97F} -arrested cells are expressed relative to WT. **(C)** NEQR cocktail-mediated rescue of cell proliferation in the face of excess Kes1 or kes1^{Y97F} (right panel) is accompanied by re-appearance of the accumulation of defective TGN/endosomal compartments which diagnose unresolved membrane trafficking defects through the TGN/endosomal system. The center panel depicts the signatures of autophagy (intra-vacuolar vesicles indicated by arrows) typical of cells producing excess Kes1/kes1^{Y97F}. **(D)** Cell cycle distribution analysis of WT cells, transformed with either YCp(P_{DOX}*::KES1*) or YCp(P_{DOX}*::kes1*^{Y97F}), grown in the presence or absence of Dox. Asynchronous cultures were fixed and stained with propidium iodide and the cell cycle distribution was determined based on genome content by FACS analysis. Error bars indicate standard deviation.

Supplemental Figure S5. Kes1 affects TORC1 signaling integrity, related to Figure 3. **(A)** *KES1* and *kes1*Δ cells were treated with 10nM rapamycin for 0-2 hours. Whole cell extracts were prepared after specified time points of rapamycin exposure and phospho-eIF2α, eIF2α (normalization control) and Kes1 were visualized by immunoblotting. *KES1* cells grown upon prolonged exposure to rapamycin show an incremental increase in phosphor-eIF2α levels. The accumulation of phospho-eIF2α in the face of rapamycin challenge is reduced in *kes1*Δ cells. **(B)** WT cells harboring YCp(P_{DOX}*::KES1*) grown in the presence or absence of dox were treated with 50nM rapamycin for 0-2 hours. Whole cell extracts were prepared after specified time points of rapamycin exposure and Phospho-eIF2α and eIF2α (normalization control) were visualized by immunoblotting. Analysis shows an incremental increase in phospho-eIF2α levels in cells grown in the presence of Dox upon prolonged exposure to rapamycin. However, cells grown in the absence of Dox possess high levels of phosphor- eIF2α prior to rapamycin treatment that persists, with no apparent increase, during exposure to rapamycin. **(C)** NEQR cocktail-mediated rescue of cell proliferation in the face of excess Kes1 or kes1^{Y97F} requires functional Gtr1 and Gtr2 GTPases. **(D)** Increased rapamycin sensitivity of Kes1 sensitized yeast. Double mutant *sec14-1*^{ts} *cki1Δ* yeast harboring either YCp(*URA3*) or YCp(*KES1*)) were grown on SC media or SC media supplemented with 5nM rapamycin. Plates were incubated at 30ºC for 72 hours.

Supplemental Figure S6. Kes1 and the sterol-binding-defective kes1^{Y97F} inhibit the GAAC, related to Figure 4. **(A)** RT-PCR of GAAC target genes (*ARG1*, *HIS4*) in cells intoxicated with either Kes1 or kes1^{Y97F} (-Dox conditions). Control conditions where

Kes1 or kes1^{Y97F} are not ectopically expressed (+Dox) serve as controls. **(B)** *ARO9* and *ARO10* expression profiles were compared in wild-type cells harboring YCp(P_{DOX}*::KES1*) cultured in the presence or absence of Dox. **(C)** Increased phospho-eIF2α levels in yeast sensitized to Kes1 activity. Immunoblots of lysates prepared from *sec14-1^{ts} cki1Δ* yeast harboring either YCp(*HIS3*) or YCp(*KES1*). Equivalent amounts of lysate were loaded and phospho-eIF2α, Kes1 and GAPDH (normalization control) were visualized by western blot analysis. **(D)** Kes1 inhibits Gcn4 derepression. β-Galactosidase assays were performed on *sec14-1^{ts} cki1Δ* yeast cells co-transformed with YCp(*GCN4::LACZ*) and either YCp(*HIS3)* or YCp(*KES1*). Error bars indicate standard deviation. **(E)** Kes1 inhibits cell growth in the presence of 3-AT. *sec14-1^{ts} cki1Δ* yeast harboring either YCp(*HIS3*) or YCp(*KES1*) were grown on SC media or SC media supplemented with 40 mM 3-AT. Plates were incubated at 30ºC for 72 hours. **(F)** Enhanced Kes1 activity (-Dox condition) abrogates Gcn4^{c}–mediated transcriptional induction (as measured by RT-PCR) of the GAAC target genes *ARG1* and *HIS4*. *ACT1* is a normalization control. Size markers (in bp) are indicated. **(G)** An NEQR cocktail restores transcriptional induction of target genes by constitutive expression of Gcn4^{c} in cells expressing excess Kes1. The experiment is designed as in (F).

Supplemental Figure S7. Sphingolipid metabolism and the GAAC, related to Figure 5. **(A)** Dual challenge of wild-type yeast with individually sub-growth inhibitory concentrations of miconazole (50ng/ml) and 3-AT (10mM 3-AT) arrests cell proliferation – indicating failure to engage the GAAC in the face of miconazole. **(B)** Mass measurements of ceramide, sphingoid base and sphingoid base phosphates in wild-type,

sec14-1^{ts} tlg2Δ, sec14-1^{ts} tlg2Δ kes1Δ cells shifted to 37ºC for 2 hrs to impose the strong *sec14-1^{ts} tlg2Δ*-associated TGN/endosomal trafficking block. **(C)** RT-PCR of the GAAC target genes *ARG1* and *HIS4* in either wild-type or *kes1Δ* cells subjected to dual 3-AT (10 mM) and PHS (7.5 μM) challenge. Neither individual challenge is growth inhibitory to wild-type yeast -- indicating failure to engage the GAAC in the face of PHS in wild-type cells. This failure is rescued by *kes1Δ* – indicating the inhibitory effects of PHS on the GAAC are Kes1-dependent. **(D)** RT-PCR analysis of *ARG1* and *HIS4* expression using total RNA fractions prepared from wild-type yeast engineered for constitutive production of Gcn4^{C} challenged with PHS. Treatment with the sphingoid base diminishes GAAC activation by Gcn4^{C} protein. **(E)** Ectopic expression of the Ypc1 ceramidase rescues GAAC activity in the face of excess Kes1 as evidenced by restoration of growth on media containing 3-AT. These experiments employed *sec14-1^{ts} cki1Δ* yeast (CTY160) which are sensitized to even mild (2X) enhancements in Kes1 activity (Fang et al., 1996). Plates were incubated at 30ºC for 72 hours. **(F)** WT yeast carrying either YEp *(URA3)* or YEp *(YPC1)* were cultured in the presence of 10mM 3-AT and increasing concentrations of PHS (0, 1, 2.5, 5 and 7.5 μM) for 15 hours and growth rates recorded. Represented are the growth rates relative to 3-AT treated cells alone.

Supplemental Table Legends

Supplemental Table S1 lists the yeast strains used in this study.

Supplemental Table S2 lists the plasmids used in this study.

Supplemental Figure S1

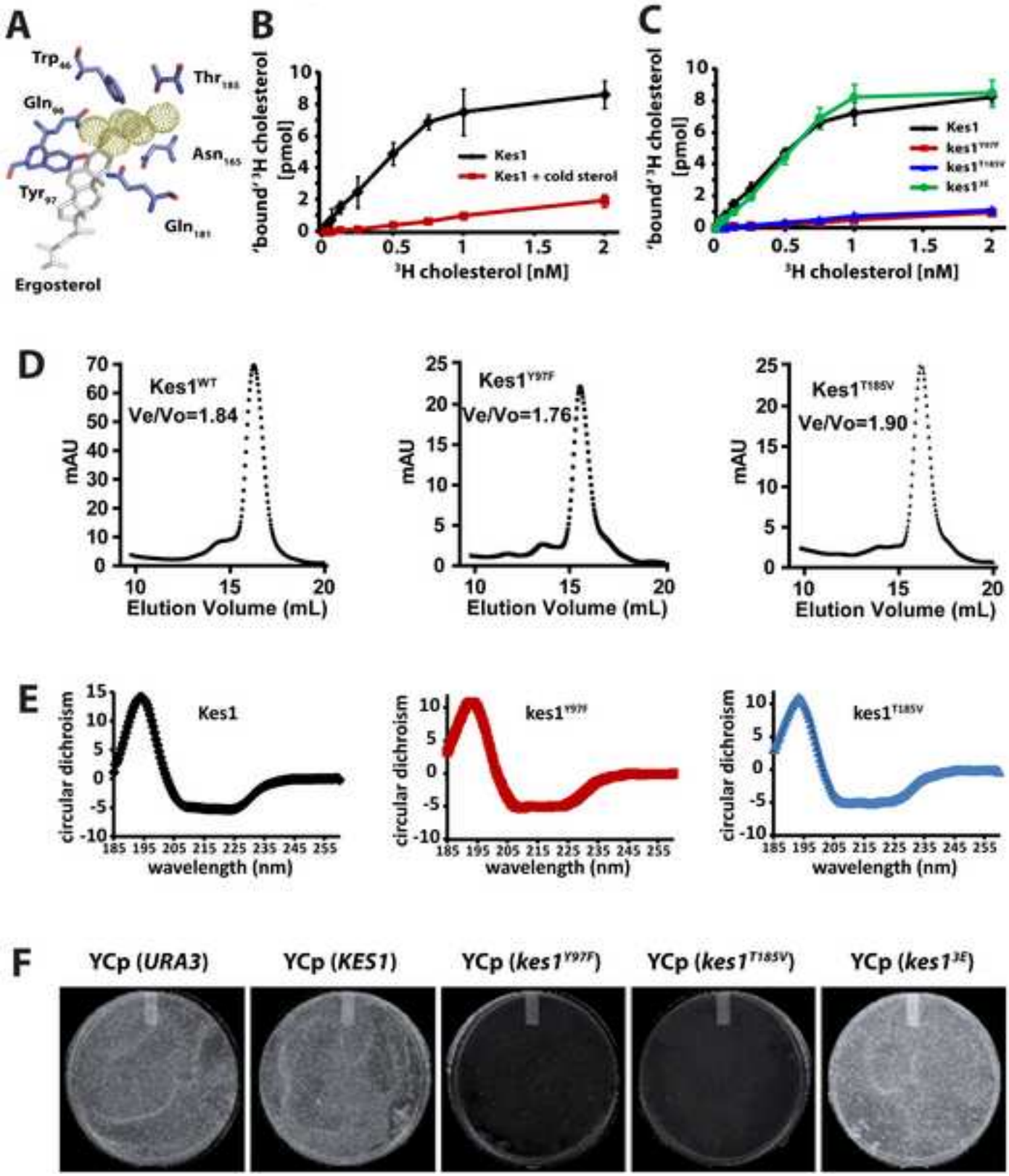

Supplemental Figure S2

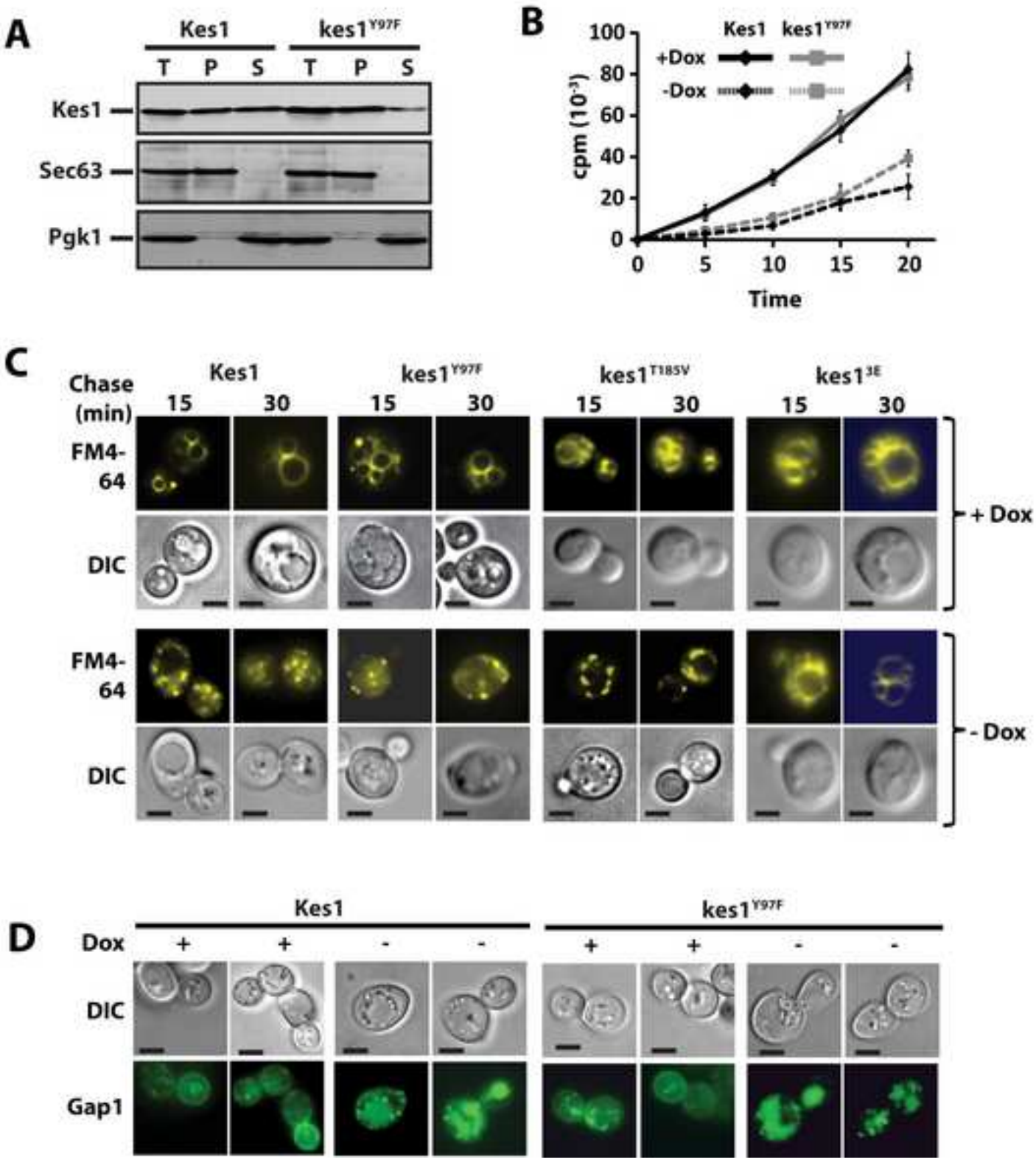

Supplemental Figure S3

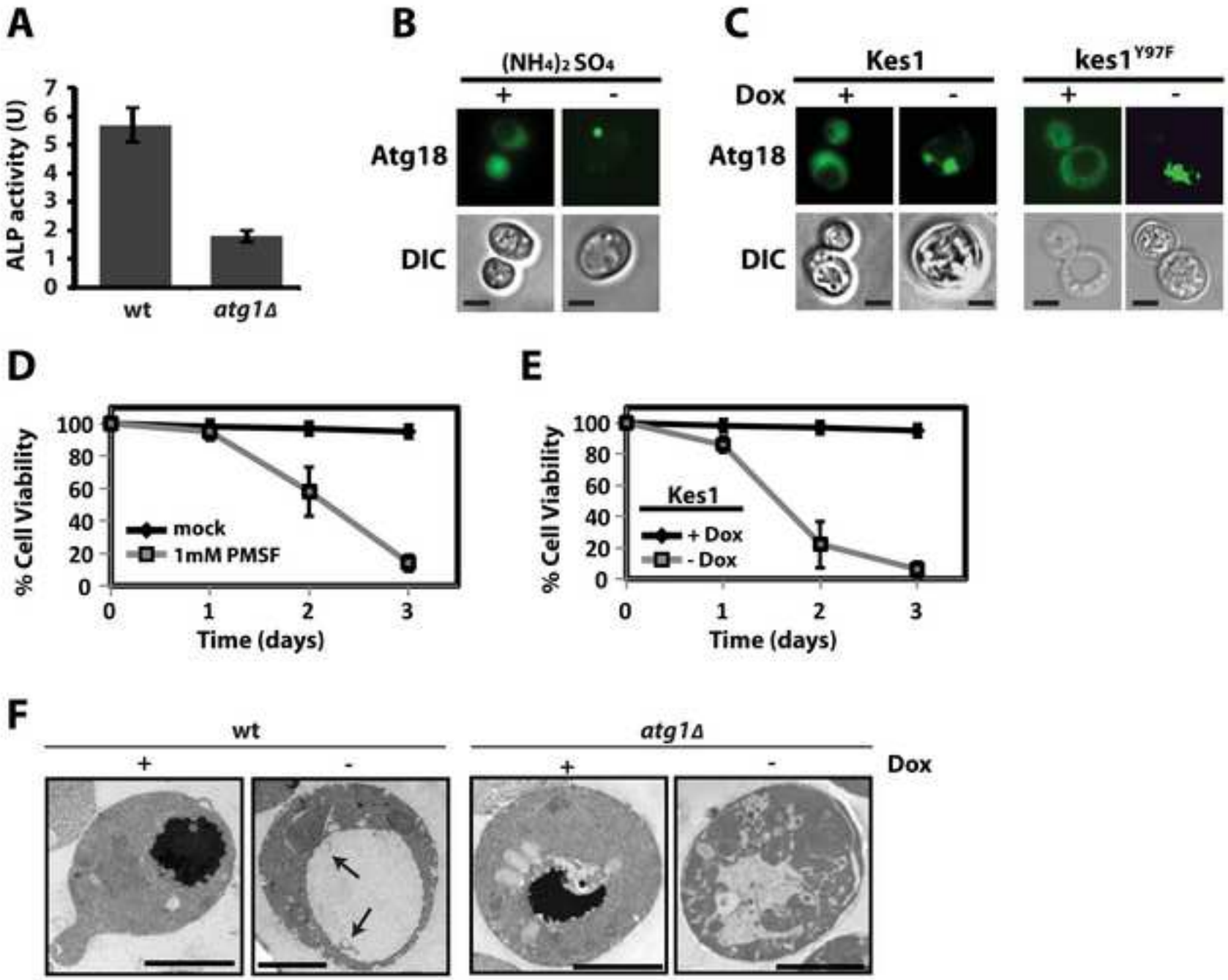

Supplemental Figure S4

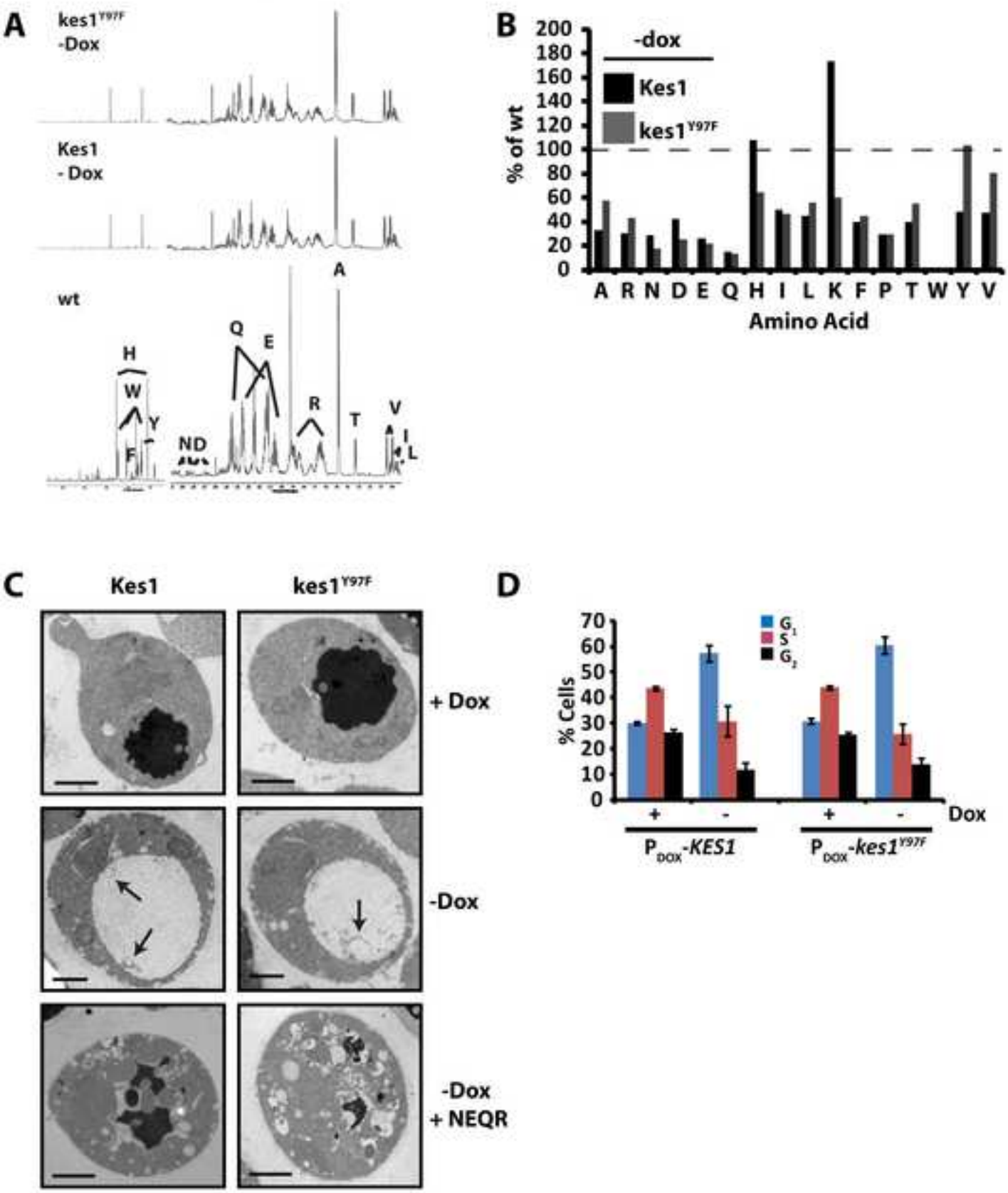

Supplemental Figure S5

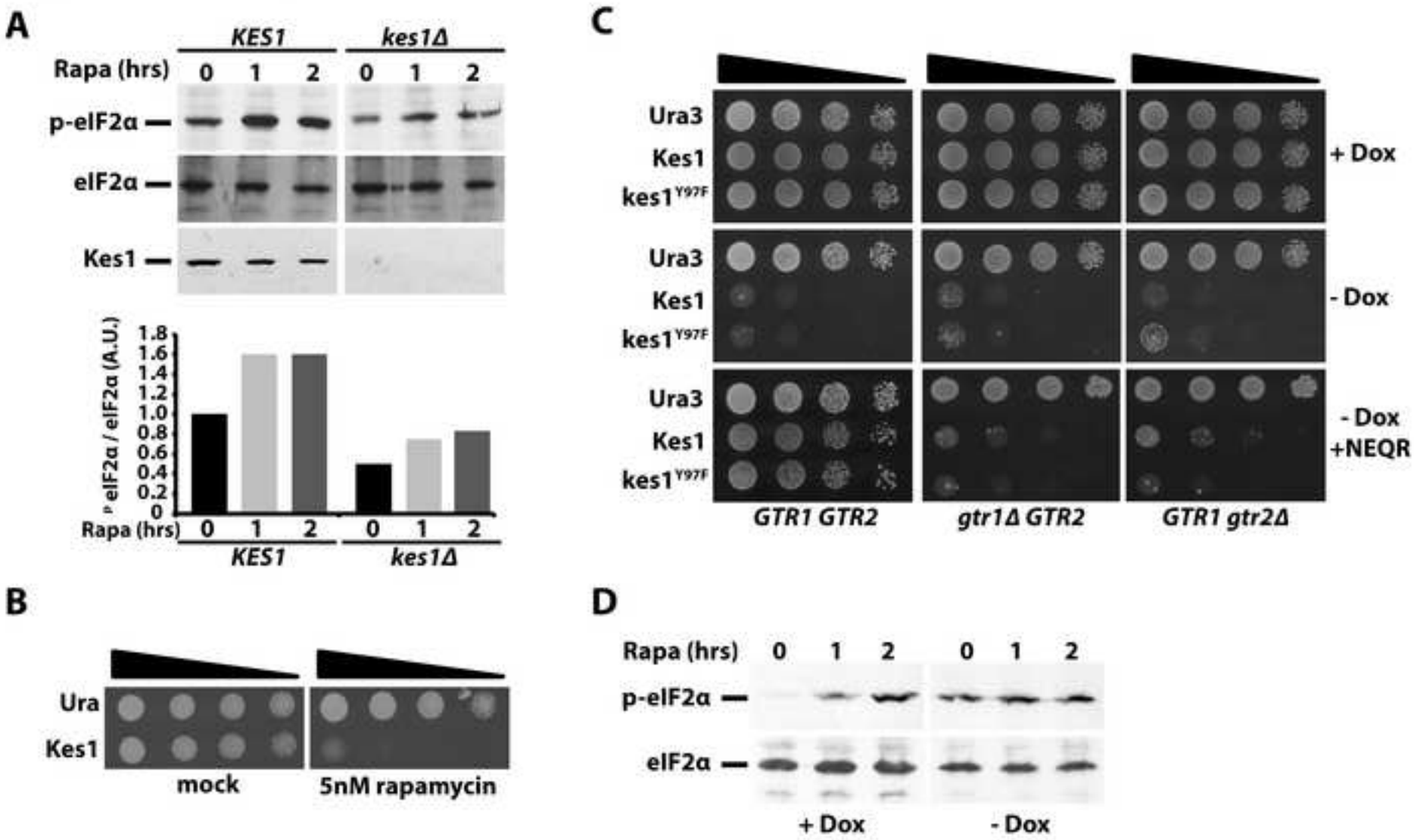

Supplemental Figure S6

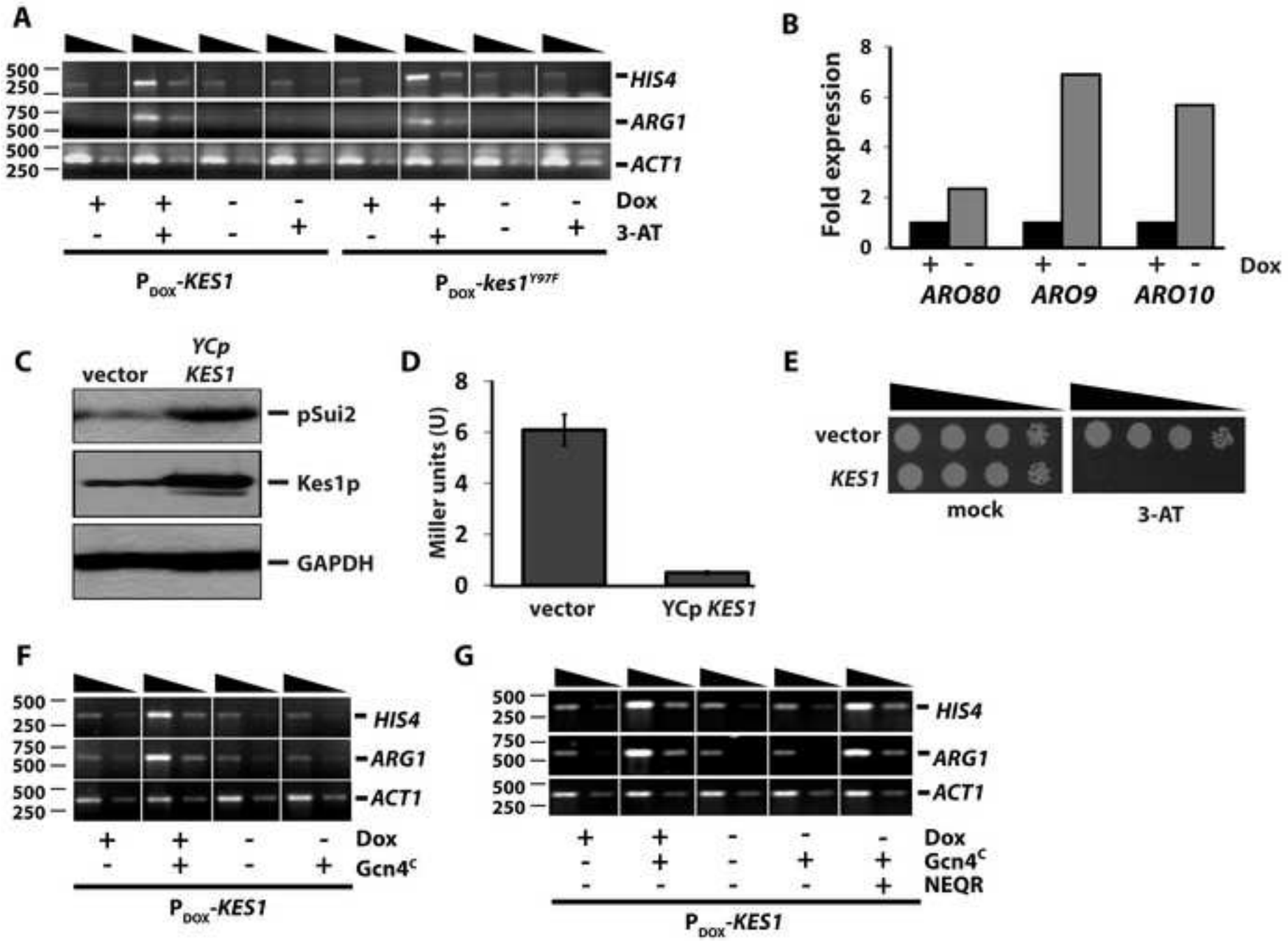

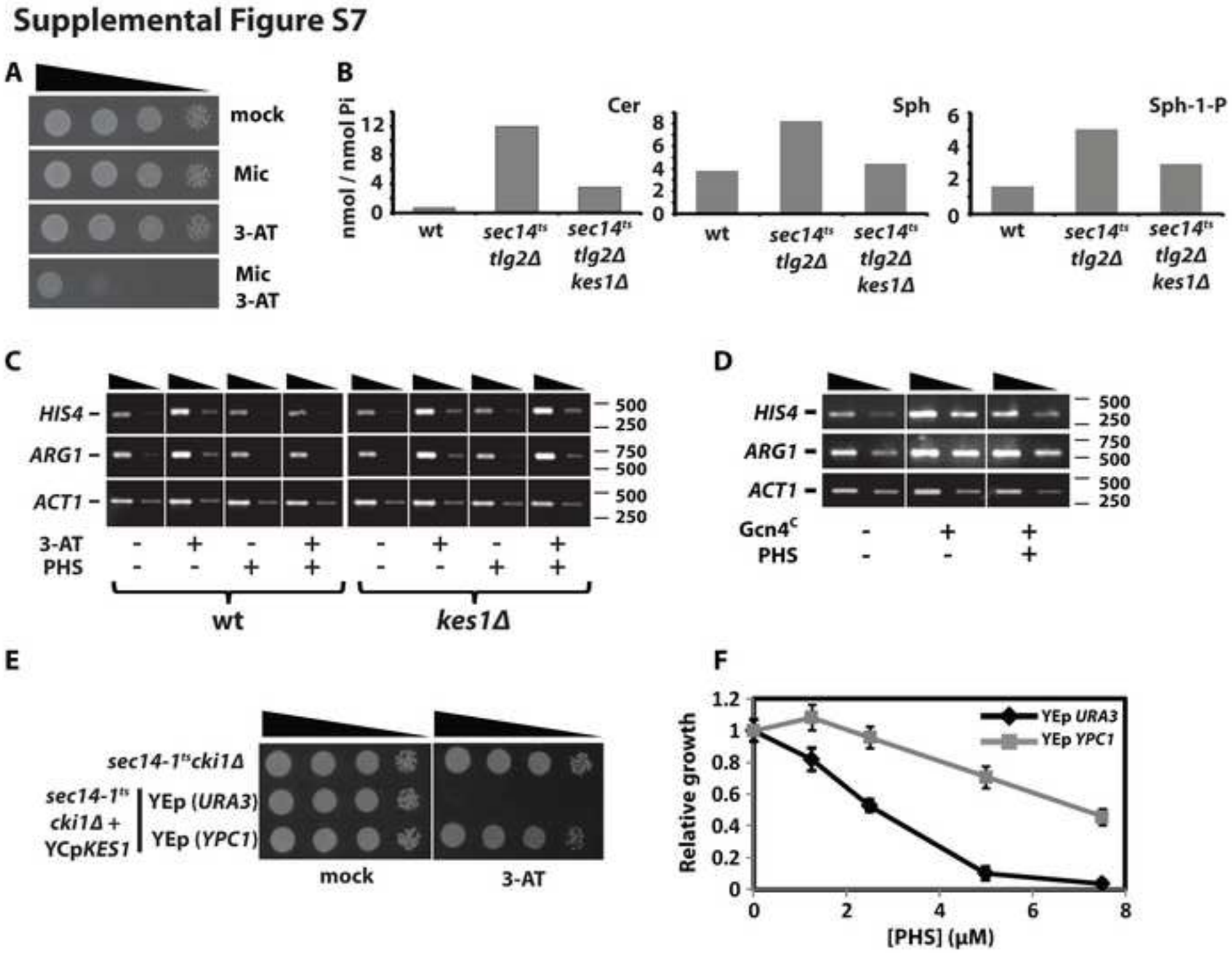
Supplemental Figure S7
A
mock
Mic
3-AT
Mic
3-AT
B
nmol / nmol Pi
Cer
Sph
Sph-1-P
wt
sec14ts tlg2Δ
sec14ts tlg2Δ kes1Δ
C
HIS4
ARG1
ACT1
500
250
750
500
3-AT
PHS
wt
kes1Δ
D
HIS4
ARG1
ACT1
Gcn4c
PHS
E
sec14-1tscki1Δ
sec14-1ts cki1Δ + YCpKES1
YEp (URA3)
YEp (YPC1)
mock
3-AT
F
Relative growth
YEp URA3
YEp YPC1
[PHS] (μM)